Journal of Solid State Electrochemistry (2020) 24:1961–1968
https://doi.org/10.1007/s10008-020-04616-z

ORIGINAL PAPER

Influence of temperature on the preparation of $CoFe_2O_4$ by the sol-gel method and its application in electrochemical energy storage

E. C. Silva[1] · J. C. M. da Costa[1] · M. C. Nascimento[1] · B. L. Pereira[1] · R. R. Passos[1] · L. A. Pocrifka[1]

Received: 11 December 2019 / Revised: 20 April 2020 / Accepted: 23 April 2020 / Published online: 7 May 2020

Abstract

$CoFe_2O_4$ particles were successfully synthesized by a sol-gel proteic route in three different temperatures, and their structural and morphological properties were studied in detail. The XRD pattern results confirmed $CoFe_2O_4$ formation with some residual second phase of αCo–Fe in low temperature calcined materials. FTIR spectra showed the strong absorption bands in the range of 440 to 650 cm^{-1}, which are related to Fe–O and Fe–Co bonds. SEM images illustrated that the cobalt ferrite particles exhibit a porous structure are formed by a hexagonal morphology. It was observed that the increase of calcination temperature resulted in more crystalline and better organized materials. $CoFe_2O_4$ specific capacity was 76.52 mA h g^{-1}at current density of 1 Ag^{-1}. This was the best result obtained with the 1000 °C material, which was based on the fact that temperature has a great influence on the electrochemical response of cobalt ferrite synthesized by proteic sol gel. It was also observed that 75% of the initial capacity remains the same for 5000 continuous cyclic voltammetry at the scan rate of 25 mVs^{-1}which confirms the superior performance of the prepared electrode as energy storage material.

Keywords Ferrites · Energy storage · Stable structure · Pseudocapacitors

Introduction

There are renewable and nonrenewable energy resources that supply existing global demand, but it is necessary to assess the limit of these resources, especially nonrenewable ones. Due to globalization, the availability of these nonrenewable sources has been decreasing, their misuse causing environmental catastrophes, and the vast majority of renewable sources are relative to the season, generating the need for materials capable of storing energy [1].

Supercapacitors are energy storage devices capable of providing fast charging, high energy density, and cycling [2]. Applications can already be found where supercapacitors replace common batteries such as chargers, tablets, and power tools.

In capacitive materials, there are two modes of energy storage, the first through electric double layer and the second by charge transfer at the electrode-electrolyte interface, which obeys Faraday's law; the second is called electrochemical pseudocapacity [3].

Currently, supercapacitors dominate research on electronic devices, and despite their widely known advantages, they have major limitations, such as low energy density, for example.

Within the group of battery-type materials, it is possible to perceive the degradation of the material during cycling, limiting the useful life of the material.

It is necessary to develop a new device that will be able to develop energy and energy of high density value. That is, the combination of battery type materials and supercapacitors.

Cobalt ferrite has been used extensively for energy storage. The use of this material is due to its excellent electrochemical properties, easy synthesis, low cost, and good theoretical capacity.

✉ L. A. Pocrifka
pocrifka@gmail.com

[1] Laboratory of Electrochemistry and Energy (LEEN), Chemistryl Graduate Program of Federal University of Amazonas (UFAM), Av. Rodrigo Otávio, 1200, Coroado, Manaus, Amazonas 69067-005, Brazil

When these materials are nanostructured, capacitive behaviors can arise as a result of the reduction of the diffusion distance and reversible intercalation ions in the structure. The total value of the capacity in this material includes capacitors and contribution of the battery type.

The study of metal oxides, such as MnO_2, IrO_2, V_2O_5, and RuO_2, has become the focus of the latest research on pseudo-capacitive devices [4–6]. As expected, electrochemical stability is only found in precious metal oxides that are often expensive in the market, so there is a need for cheaper, less toxic, and more stable materials. Transition metal oxides have been widely studied as an electrode material of pseudocapacitors due to its potentially high discharge capacity and high energy density [3].

In this context, the study between mixed metal oxides such as ferrite is able to provide chemical stability and useful chemical properties for application. Several spinel ferrites, including $MnFe_2O_4$, $ZnFe_2O_4$, $CoFe_2O_4$, and $NiFe_2O_4$, have been used as working electrodes for energy storage [7–9].

Depending on the form of synthesis, these materials may be suitable for various applications such as energy storage devices, magnetic materials, gas sensors, catalysts, photocatalysts and absorbent materials, among others [10–12].

The sol-gel method is based on inorganic polymerization reactions. It includes four steps as follows: hydrolysis, polycondensation, drying, and thermal decomposition. Calcination at higher temperature is needed to decompose almost completely the organic precursor. The size of the sol particles depends on the solution composition and temperature. By controlling these factors, one can tune the size of the particles [13].

The major advantages of sol-gel processing for optical and electronic applications are as follows: (i) ambient temperature of sol preparation and gel processing; (ii) product homogeneity; (iii) low temperature of sintering; (iv) ease of making multi-component materials; and (v) good control over powder particle size and shape as well as size distribution [14].

The sol-gel proteic process, is composed by a sol, that is a stable dispersion composed of colloidal particles in a solvent, which with increasing system energy tends to evolve into a three-dimensional configuration, and a gel that is composed of a polymer that gives the solution gelatinous consistency [13, 14]. In this synthesis, in order to reduce environmental aggression, we use eatable gelatin as a polymeric material.

This research aims to obtain $CoFe_2O_4$ particles through an environmentally friendly and inexpensive synthesis, with particle size and controlled properties from temperature variation, to understand its influence on the material's energy storage capacity and its cyclability.

Experimental section

To perform the synthesis, 2 g of commercial tasteless gelatin, 1 g of cobalt chloride ($CoCl_2.6H_2O$), and 1 g of iron chloride ($FeCl_2.6H_2O$), both of the Sigma Aldrich, were mixed in 200 mL of distilled water; 20 mL of KOH 1molL^{-1} solution are added to enable solution hydrolysis.

This mixture was homogenized at a temperature of approximately 50 °C under constant stirring for 50 min. The material was dried at approximately 100 °C for 24 h and calcined for 2 h, at three study temperatures as follows: 600, 800, and 1000 °C. This temperature variation will allow the evaluation of these material's performances from the result of their properties.

Characterization techniques

The obtained materials were characterized by X-Ray diffraction using a Shimadzu X-Ray diffractometer model XRD 7000 with CuKα radiation ($\lambda = 1.54056$ Å). The diffractograms were recorded in 2θ in the range of 25 to 70°, with step size of 0.05° and scan time of 2 s per step.

Scanning electron was recorded using a microscope model Vega3 Tescan. The sample preparation was carried out by fixing the calcined powder on a carbon tape superimposed on an aluminum stub. The sample was previously metallized in a Bal-Tec SCD 050 Sample Sputter Coater.

The Fourier-transform infrared spectra (FTIR) were recorded in the region 3000–380 cm^{-1} using Perkin–Elmer spectrum 100 spectrophotometer using ATR indictor to determine the vibrational structures of the prepared materials.

The electrochemistry characterization was carried out using a film prepared by binder method, where the ratios of active material, Carbon Vulcan, and Nafion followed the ratio of 70:25:5 on stainless-steel 304 substrate; as the working electrode, they were prepared for a mass of approximately 0.8 mg of deposited material, a platinum wire as the counter electrode, and an Ag/AgCl/saturated KCl as the reference electrode.

The prepared electrodes had a mass equivalent to 0.7641, 0.8134, and 0.7950 g for calcination temperatures of 600, 800, and 1000 °C, respectively. All were deposited on a metallic substrate with an area of 1×0.5 cm^2.

A solution of 1.0 molL^{-1} KOH was used as electrolyte. Cyclic voltammograms were performed in a potential range between − 1.3 and − 0.3 V at different scan rates, ranging from 1 to 200 mVs^{-1}.

The galvanostatic charge-discharge (GCD) cycles were recorded within a potential range of − 1 to 0 V at 1 Ag^{-1}. The spectra of impedance electrochemistry were collected in the frequency range from 0.1 to 10.000 Hz in 10 mV of open circuit.

All the electrochemical measurements were conducted using an Autolab Potentiostat (PGSTAT 302 N).

Results and discussion

Structural and morphological analysis

In Fig. 1a, the X-ray diffractograms of $CoFe_2O_4$ samples treated at temperatures of 600, 800, and 1000 °C was illustrated. In diffractograms, it is possible to observe that, as temperature, the peaks become more intense and narrower, which indicates greater crystallinity in the material [15]. The presence of the cobalt ferrite crystalline phase ($CoFe_2O_4$–JCPDS 22–1086) was identified, and the lattice constants are 8.4743 Å, 8.4751 Å, and 8.4610 Å for 600, 800, and 1000 °C, respectively, which agree with standard data. For all samples, the $CoFe_2O_4$ crystalline phase was predominant. In samples calcined at 600 and 800 °C, it is possible to observe the remaining presence of the αCo–Fe phase, according to the JCPDS 65–6829. The presence of this phase justifies the change of the crystallite size and may influence the electrochemical performance of the materials.

The crystallite size of the three materials was determined using the Scherrer eq. 1:

$$D = \frac{0.9\lambda}{\beta cos\theta} \quad (1)$$

where λ is the wavelength of the X-rays emitted by the target, θ is the Bragg diffraction angle, and β is the full width at half the maximum intensity. The crystallite size of the nanostructured $CoFe_2O_4$ at 600, 800, and 1000 °C was found at about 21, 26, and 31 nm for the plane (3 1 1).

Increasing synthesis temperature reduces synthesis residues, like organic material from gelatin, and improves material crystallinity and structural organization. The crystal growth with the temperature increase observed in this work is comparable with that observed by Yuqiu Qu et al., who also reported that the sharpness of the prominent peak increases as the grain size of nanomaterials grow [16].

The FT-IR spectrum of $CoFe_2O_4$ nanomaterials in the range of 3000–380 cm^{-1} is shown in Fig. 1b. The spectrum supports

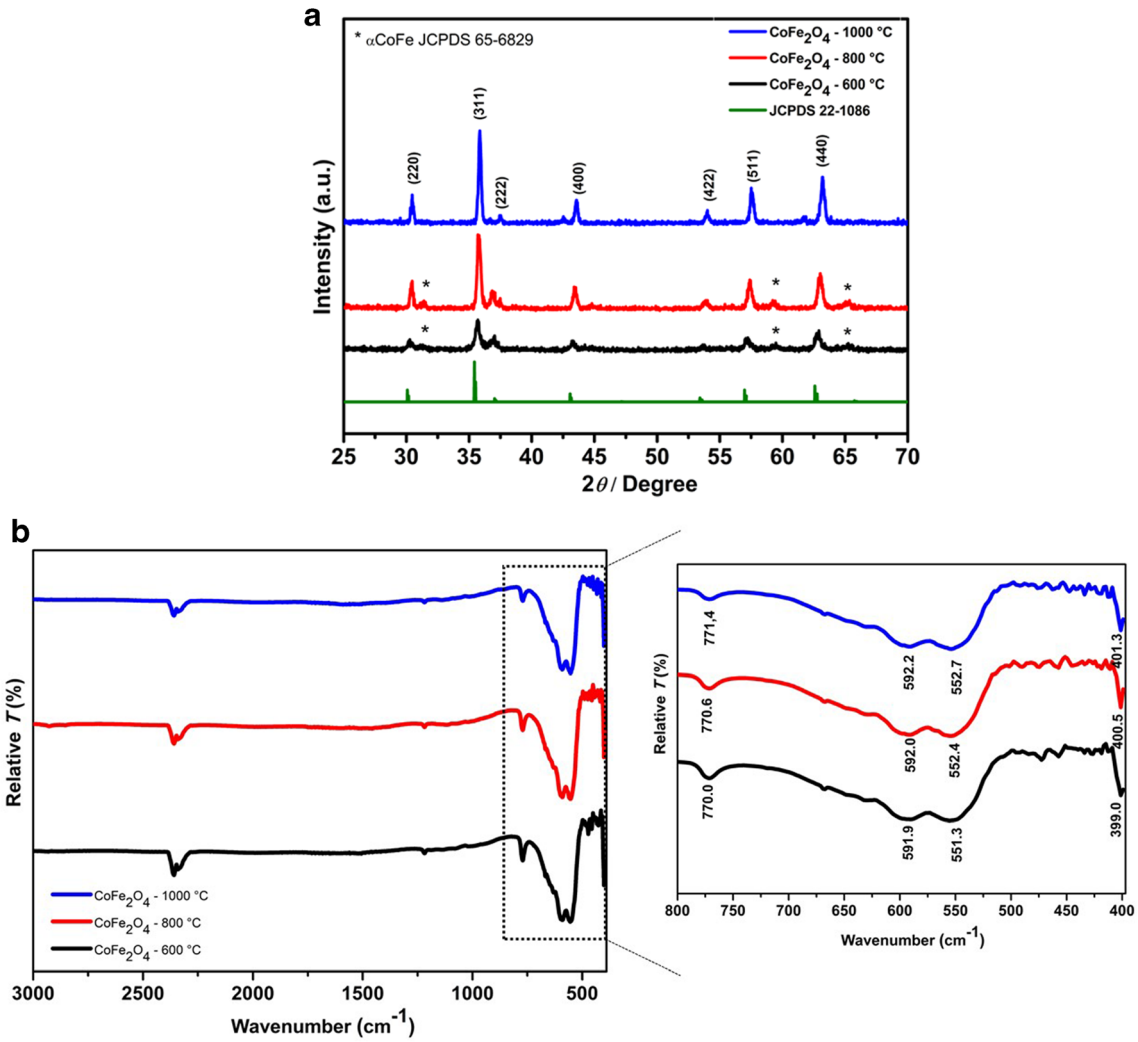

Fig. 1 **a** X-ray diffraction patterns of $CoFe_2O_4$ powder. **b** The FT-IR pattern of $CoFe_2O_4$ material

the formation of spinel structured $CoFe_2O_4$. The typical inverse spinel ferrite structure consists of two IR absorption bands, one at around 400 cm^{-1}, which attributes to the stretching vibration of tetrahedral groups Fe^{3+} O^{2-}, and other at around 600 cm^{-1}, representing octahedral group complex Co^{2+} O^{2-} [17]. In the present study, the bands mentioned above appear at around 392 and 570 cm^{-1}, respectively, which indicate the presence the formation of $CoFe_2O_4$. Similar results were reported in the work by authors like Shirsath et al. [18]. The FTIR analysis results are analogous to the results obtained from XRD.

Figure 2 shows SEM images of calcined $CoFe_2O_4$ synthesized nanomaterials by the proteic sol-gel method at three different temperatures; the materials exhibit a hexagonal morphology, as reported in the work of Shirsath et al. [18], with more expensive and complex synthesis processes than presented in this paper. A structurally improved material is believed to be beneficial for interaction with the electrolyte, leading to improved electrochemical reactions [18]. It is possible to observe in microstructures that materials become better organized on the surface when treated at higher temperatures. This is consistent with the previously reported studies [18, 19].

Electrochemical performance of $CoFe_2O_4$ materials

Cyclic voltammetry study

CV curves of $CoFe_2O_4$ at different scan rates are shown in Fig. 3a, b, and c for calcined materials at 600 °C, 800 °C, and 1000 °C, respectively. In the voltammograms, it is possible to observe a pair of redox peaks around − 1 V and − 0.6 V, which indicates the battery behavior of the materials [18]. The displacement of the peaks with the increase of the scan rate is explained by the polarization effect of the material electrode at high rates. The reduction peak correspond to the conversion reaction of Fe^{3+} and Co^{2+} to their metallic states and oxidation peak is attributed to the oxidation of Fe and Co to Fe^{3+} and Co^{2+}, respectively.

The electrochemical semi-reaction of this process is indicated in the eq. (2) below:

$$CoFe_2O_4 + H_2O + OH^- \leftrightarrow CoOOH + 2FeOOH + e^- \quad (2)$$

As the synthesis temperature increases, the reversibility of redox processes can be improved. Figure 3 shows that by applying a scan rate variation from 1 to 200 mVs^{-1}, there is a reduction in the distance of the anodic and cathodic peaks. This fact occurs due to the higher crystallinity and morphology of the calcined material at higher temperature; these properties improve interaction with the electrolyte and ion diffusion [16]

A calculation was performed to obtain the equivalent *R* of the slope of the lines from the maximum current values of the cathode peaks of the voltammograms shown in Fig. 3a–c. The reversibility lines for each set of voltammograms showed the following values for *R*: 0.994, 0.996, and 0.998, for the temperatures 600, 800, and 1000 °C respectively. The *R* value of a

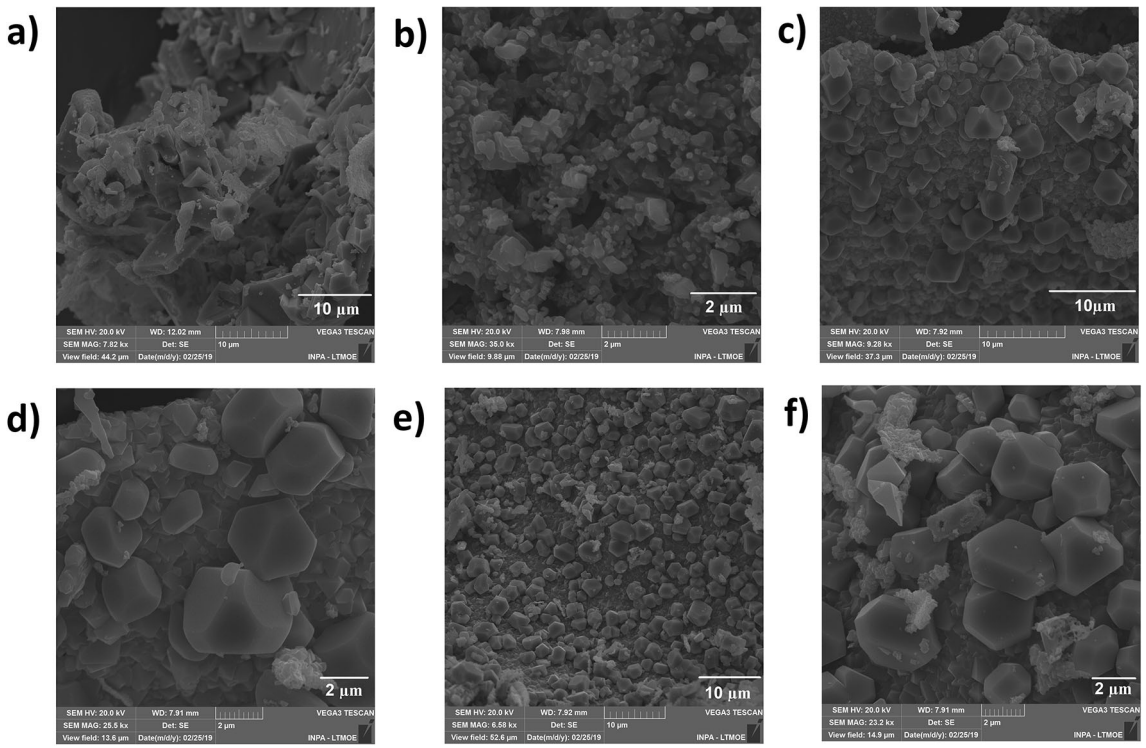

Fig. 2 SEM images for all three materials at scale levels 2 µm and 10 µm. **a** and **b** 600 °C; **c** and **d** 800 °C; **e** and **f** 1000 °C

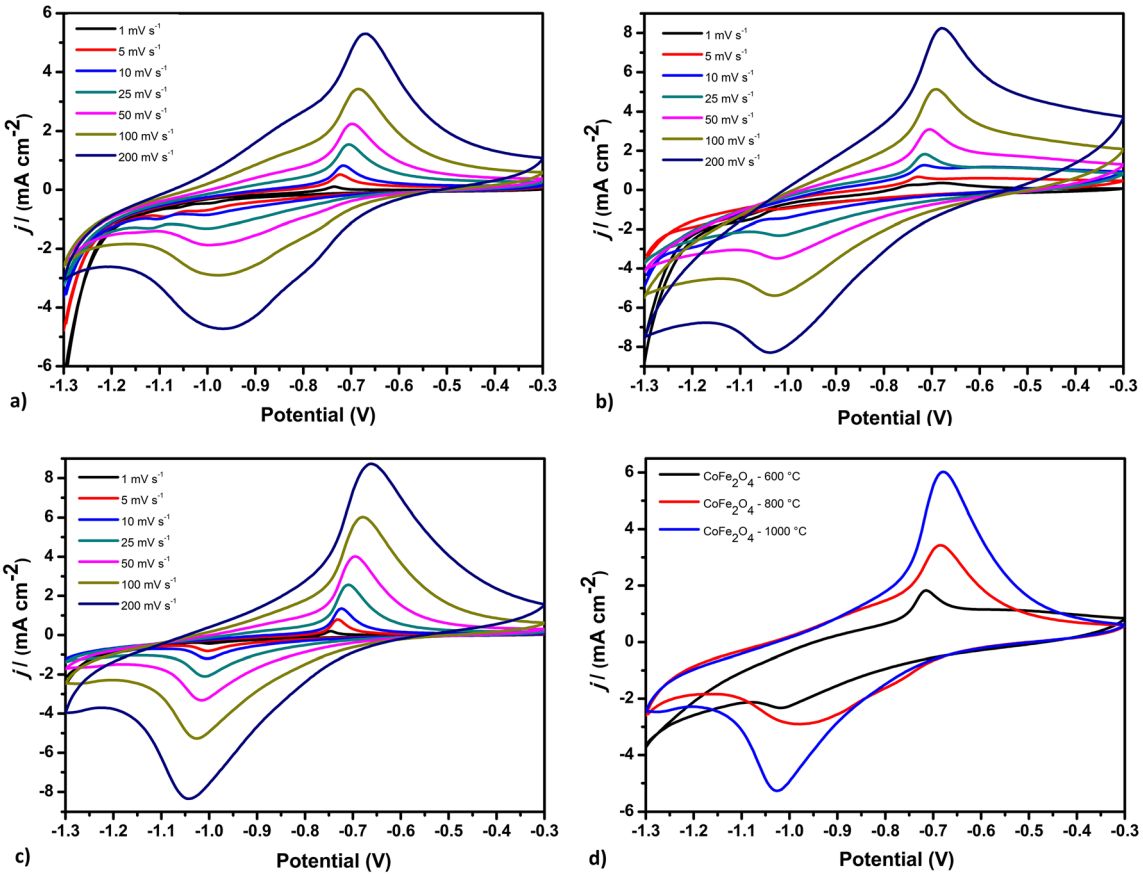

Fig. 3 Cyclic voltammetry curves of $CoFe_2O_4$ electrodes at different scan rates from 1 to 200 mV s^{-1} within a voltage window of 0.1 to 0.6 V. **a** Calcined material at 600 °C. **b** Calcined material at 800 °C. **c** Calcined material at 1000 °C. **d** $CoFe_2O_4$ cyclic voltammetries curves at different calcination temperatures at 25 mV s^{-1} scan rate

line indicates its linearity, when closer to 1, and in this case, it indicates the highest reversibility of the applied materials.

The advantage of increased surface in calcined materials expands electrochemical activity and reversibility, as seen in Fig. 3a–c. As a result, with the increase in the calcination temperature, an electrode with higher electrical conductivity, more reversible, and therefore with longer lifespan is obtained.

The capacity values relate to different material at 25 mV were clearly observed in Fig. 3d, where values of 137.91, 102.58, and 43.27 mA hg^{-1} were obtained for materials of 1000, 800, and 600 °C, respectively.

The obtained results were consistent with those reported by other researches [15, 16, 18, 20] and even more encouraging considering that the material is synthesized by a simple, cheaper, and environmentally friendly route.

Charge–discharge study

To calculate the specific capacity of the $CoFe_2O_4$ electrodes, the galvanostatic charge and discharge (GCD) measurements were performed with a potential range from − 1.0 to 0 V with current density in 1 to 10 Ag^{-1}.

GCD curves for the three $CoFe_2O_4$ materials are shown in Fig. 4a, b. The capacity values relate to different current densities, calculated by eq. (4) where I is the current density, Δt is the discharge time, and m is the mass of active material (3):

$$C = \frac{I \cdot \Delta t}{m} \tag{3}$$

In this work, it is possible to observe in Fig. 4a the capacity values for each current density used; the values decrease with the current increase according to a battery type material. Figure 4b shows typical GCD curves of $CoFe_2O_4$ at current density of 1 Ag^{-1}. The results obtained were 76.52, 14.74, and 6.58 mA h g^{-1} for materials of 1000, 800, and 600 °C respectively. These results are consistent with those found in the literature, as in the works by Ramakrishnan et al. [18].

The stability of the materials is shown in Fig. 4c where it is possible to see better performance of the calcined material at 1000 °C due to less wear of the redox sites of the material. This characteristic is attributed to the increase of reversibility that the materials present with the increase of the synthesis temperature.

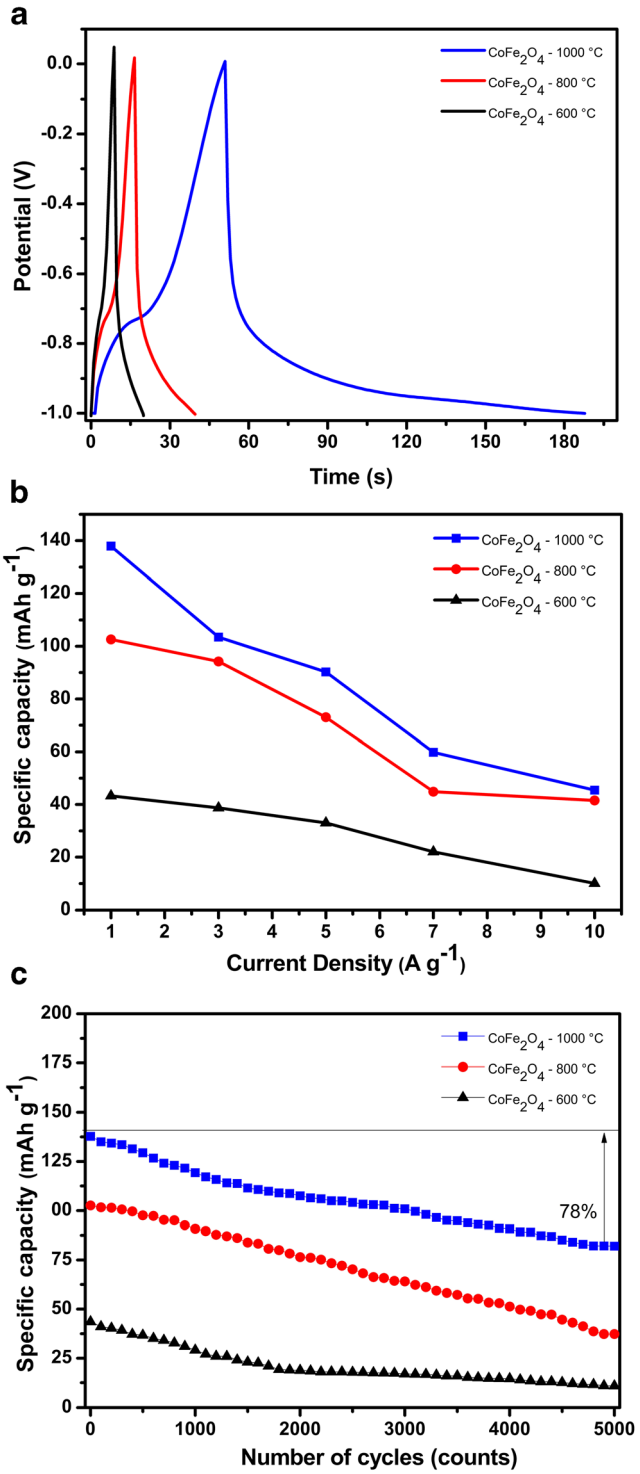

Fig. 4 **a** Galvanostatic charge–discharge recorded at 1 Ag^{-1} for the $CoFe_2O_4$ film. **b** Capacity of $CoFe_2O_4$ as function of the number cycle calculated from GCD curves. **c** Electrochemical stability data performed at 25 mVs^{-1} in voltammetry cycles

The stability test was performed by 5000 cycles of cyclic voltammetry, performed in 1 M KOH electrolyte at 25 mVs^{-1} scan rate. The $CoFe_2O_4$ material exhibits long-term cyclic stability with the capacity loss of 22% over 5000 cycles. This is comparable, and in some cases, an improvement on reported values for similar materials, as observed in the works of Wang et al. [19] and Ruibin et al. [21].

The capacity loss in this study may be due to the decrease of electrolyte ions and loss of electrical contact between active material and the substrate. The charge-discharge curves maintain the symmetric and linear charge-discharge behavior, revealing good electrochemical reversibility of the device.

Spectroscopy impedance study

Through the analysis (Fig. 5) of the Nyquist graphs, which observed the different behaviors of $CoFe_2O_4$, capacitive performances were observed for all materials, with certain particularities. The material synthesized at 1000 °C presented a curve close to 90°, at temperatures of 800 and 600 °C; despite demonstrating capacitive behaviors, they have different inclinations by Nyquist, and this is due to the difference in the crystallinity level obtained in the structures [22, 23], as observed in diffractograms, and being confirmed by SEM images, since $CoFe_2O_4$ at 1000 °C has a more uniform and well-distributed structure when compared with temperatures of 800 and 600 °C.

These assumptions were proved by the electrochemical analysis by CV and GCD, where the 1000 °C voltammetry curve obtained a higher performance behavior in the anodic and cathodic profiles, compared with the other two synthesis temperatures (800 and 600 °C), and in the GCD, the longest discharge time was for $CoFe_2O_4$ at 1000 °C.

The analyses by Bode graphs (Fig. 5b) performed an evaluation as a function of the frequency of $CoFe_2O_4$ obtained at different synthesis temperatures at 45° angle, which corresponds to the material relaxation time $\tau_0 = \frac{1}{2f}$; this constant corresponds to the minimum time required to discharge all energy from the material with an efficiency greater than 50% [24–26].

Performing such evaluations at 45° angle for all materials, the values of different relaxation constants obtained in the high frequency region were τ_0 of 0.16, 0.05, and 0.33 *ms* for the temperatures of 600, 800, and 1000 °C; it is worth mentioning that analysis is performed at 45° angulation frequencies; however, when looking at the phase angle formation, the materials reached the following angles 81° to 1000 °C, 79° for the synthesis performed at 800 °C, and 61° for $CoFe_2O_4$ obtained at 600 °C; such observations are consistent with the behaviors shown by the Nyquist plot.

Conclusions

Spinel cobalt ferrite particles with grain size of 21 ~ 31 nm have been synthesized by a proteic sol-gel method. XRD and MEV characterizations confirmed the phase of cubic $CoFe_2O_4$. The electrochemical properties of $CoFe_2O_4$

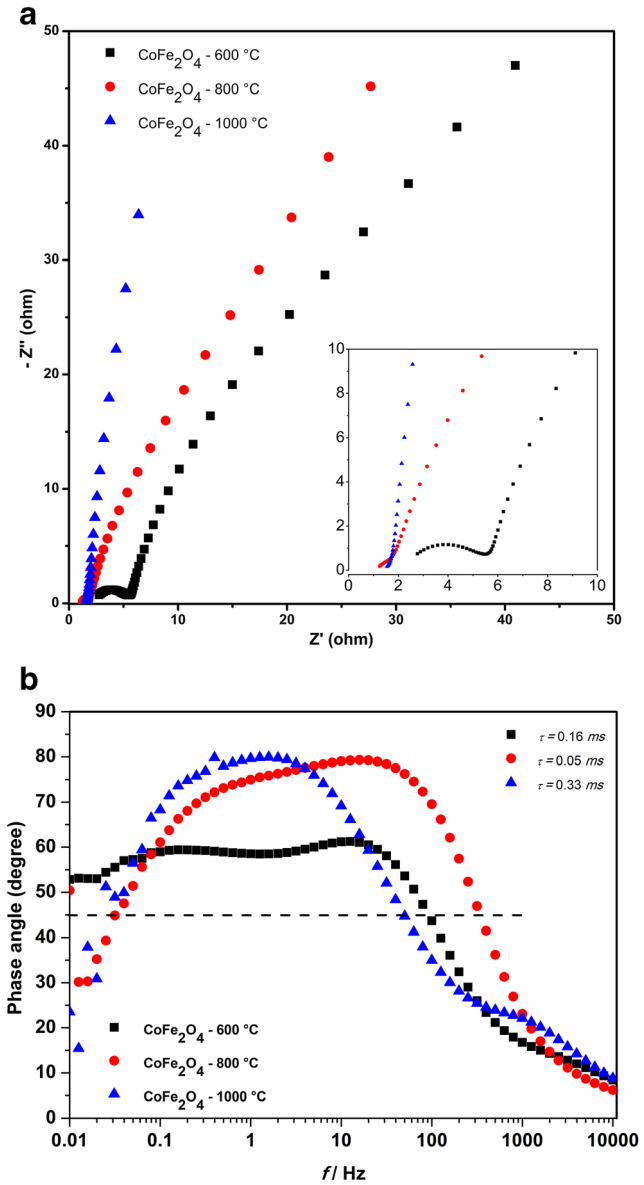

Fig. 5 **a** Nyquist plots (−Z'' vs. Z') of $CoFe_2O_4$ nanomaterials in 1 M KOH solution. **b** Bode plot of the $CoFe_2O_4$ nanomaterial

nanomaterials have been evaluated though cyclic voltammetry, EIS, and galvanostatic charge/discharge cycling tests. It was observed that the increase of calcination temperature resulted in more crystalline and better organized materials.

The $CoFe_2O_4$ specific capacity was 76.52 mA h g^{-1} at a current density of 1 A g^{-1}. This result comes from the calcined material at 1000 °C, which is consistent with several studies cited throughout the work. The results indicate that $CoFe_2O_4$ when prepared by the sol-gel method at high temperatures has the best values of capacity, reversibility, and cyclability.

This research shows the possibility of producing stable cobalt ferrites through a simpler and more environmentally friendly route, obtaining a material with the necessary stability to a good performance as an energy storage material.

Funding information The authors would like to thank the Brazilian research funding institution FAPEAM for their support and to the Laboratório Temático de Microscopia Óptica e Eletrônica (INPA) for the SEM images.

References

1. Ander G, Eider G, Jon AB, Roman M (2016) Review on supercapacitors: technologies and materials. Renew Sust Energ 58:1189–1206
2. Conway BE (1999) Electrochemical Supercapacitor: Scientific Fundamentals and Technological Applications. Springer Science and Business Media, New York
3. Shengwen Z, Chuang P, Kok CN, George ZC (2010) Nanocomposites of manganese oxides and carbon nanotubes for aqueous supercapacitor stacks. Electrochim Acta 55:7447–7453
4. Dong-Qiang L, Sung-Hun Y, Se-Wan S, Seung-Ki J (2008) Electrochemical performance of iridium oxide thin film for supercapacitor prepared by radio frequency magnetron sputtering method. ECS Trans 16:103–109
5. Grace W, Huan ZS, Yan LC, Subodh GM, Madhavi S (2010) Synthesis and electrochemical properties of electrospun V_2O_5 nanofibers as supercapacitor electrodes. J Mater Chem 20:6720–6725
6. Chi-Chang H, Kuo-Hsin C, Ming-Champ L, Yung-Tai W (2006) Design and tailoring of the nanotubular arrayed architecture of hydrous RuO_2 for next generation supercapacitors. Nano Lett 6:2690–2695
7. Venkata C, Manorama S (1999) Reddy semiconducting gas sensor for chlorine based on inverse spinel nickel ferrite sensors actuators. Sensors Actuators B Chem 55:90–95
8. Michael GC, Shan XW (2006) Room-temperature spin filter in a $CoFe_2O_4/MgAl_2O_4/Fe_3O_4$ magnetic tunnel barrier - physical review. B 74:14418
9. Matthew JC, Stefan M, Philip MR, Robin FCF, Andrew K (2002) Spin valves using insulating cobalt ferrite exchange-spring pinning layers. Appl Phys Lett 81:1044–1046
10. Wolf SA, Awschalom DD, Buhrman RA, ChtchelkanovaA Y, Treger DM (2001) Spintronics: a spin-based electronics vision for the future. Science 294:1488–1495
11. Dimos D, Mueller C (1998) Perovskite thin films for high-frequency capacitor applications. Annu Rev Mater Sci 28(1):397–419
12. James T, Thomas H (2006) A comparison of the underwater acoustic performance of single crystal versus piezoelectric ceramic-based "cymbal" projectors. J Acoust Soc Am 119:879–889
13. Chun-Ye Z, Xiang-Qian S, Jian-Xin Z, Mao-Xiang J, Kai C (2007) Preparation of spinel ferrite $NiFe_2O_4$ fibres by organic gel-thermal decomposition process. J Sol-Gel Sci Technol 42:95–100
14. Hongtao C, Yanyan J, Wanzhong R, Wenhua W (2010) Facile and ultra large scale synthesis of nearly monodispersed $CoFe_2O_4$ nanoparticles by a low temperature sol-gel route. J Sol-Gel Sci Technol 55:36–40
15. Mathew G, Swapna SN, Malini A, Anantharaman P (2007) Finite size effects on the electrical properties of sol-gel synthesized $CoFe_2O_4$ powders: deviation from Maxwell–Wagner theory and evidence of surface polarization effects. J Phys D Appl Phys 40:1593–1602
16. Yuqiu Q, Haibin Y, Nan Y, Yuzun F, Hongyang Z, Guangtian Z (2006) The effect of reaction temperature on the particle size, structure and magnetic properties of coprecipitated $CoFe_2O_4$ nanoparticles. Mater Lett 60:3548–3552
17. Vadivel B, Ramesh BR, Sethu R, Kandasamy R, Mukannan A (2014) Synthesis, structural, dielectric, magnetic and optical

properties of Cr substituted $CoFe_2O_4$ nanoparticles by co-precipitation method. J Magn Magn Mater 362:122–129
18. Shirsath E, Jadhav S, Mane L, Li S (2016) Ferrites obtained by sol–gel method. Handbook of Sol-Gel Science and Technology, 1–41
19. Liang H, Laifa S, Jie W, Yunling X, Xiaogang Z (2016) Hollow $NiCo_2S_4$ nanotube arrays grown on carbon textile as a self-supported electrode for asymmetric supercapacitors. RSC Adv 6: 9950–9957
20. Michaela SB, Matthew GK, Lena T, Adam MS, Shannon WB (2015) Cobalt-iron (oxy)hydroxide oxygen evolution electrocatalysts: the role of structure and composition on activity, stability, and mechanism. J Am Chem Soc 137:3638–3648
21. Qiang R, Hu Z, Yang Y, Li Z, An N, Ren X, Hu H, Wu H (2015) Monodisperse carbon microspheres derived from potato starch for asymmetric supercapacitors. Electrochim Acta 167:303–310
22. Guo-Qing Z, Yong-Qing Z, Feng T, Hu-Lin L (2006) Eletrochemical characteristics and impedance spectroscopy studies of nano–cobalto silicate hydroxide for supercapacitor. J Power Sources 161:723–729
23. Luciena F, Thayse S, Jakeline R, ViniciusS RR, Marco AM, Daniel AM (2019) Structure, magnetic behavior and OER activity of $CoFe_2O_4$ powders obtained using agar – agar from red seaweed (*Rhodophyta*). Mater Chem Phys 237:121847
24. Hongyan G, Shaokui C, Yan C (2017) Hierarchical core-shell nanosheet arrays with MnO2 grown on mesoporous CoFe2O4 support for high-performance asymmetric supercapacitors. Electrochim Acta 240:31–42
25. Ga H, Shaokui C, Yan C (2013) Complex impedance with transmission line model and complex capacity analysis of ion transport and accumulation in hierarchical core-shell porous carbons. J Electrochem Soc 160:H271–H278
26. Shuijian H, Wei C (2015) Application of biomass – derived flexible carbon cloth coated with MnO_2 nanosheets in supercapacitors. J Power Sources 294:150–158